Exploratory Research and Hypothesis in Medicine **2022** vol. 7(4) | 228–240
DOI: 10.14218/ERHM.2021.00048

Original Article

Identification of Omentum-derived Molecular Determinants and Pathways Mediating the Omental Metastasis of Ovarian Cancer

Meifeng Zhou[1], Li Sheng[1], Haixia Wang[1], Xufeng Zhang[2], Jindian Tan[3*] and Lin Wang[1*]

[1]Department of Medical Oncology, Hainan General Hospital, Hainan Affiliated Hospital of Hainan Medical University, Haikou, China; [2]Cancer Center, the First Affiliated Hospital of Hainan Medical College, Hainan Medical College Cancer Institute, Haikou, China; [3]Department of Orthopaedic Surgery, Hainan General Hospital, Hainan Affiliated Hospital of Hainan Medical University, Haikou, China

Received: September 28, 2021 | **Revised:** October 22, 2021 | **Accepted:** January 10, 2022 | **Published:** March 18, 2022

Abstract

Background and objectives: To date, the omentum-derived determinants of ovarian cancer (OC) metastasis to the omentum have not been well elucidated. We aimed to identify the pathogenesis, potential biomarkers, and prognostic indicators underlying the omental metastasis of OC.

Methods: The expression profile GSE120196 included datasets of omental tissues from four patients with benign gynecologic diseases and cancer-infiltrated omental tissues from ten patients with high-grade serous OC. Using this dataset, we performed an analysis of differentially expressed genes (DEGs), gene ontology, Kyoto Encyclopedia of Genes and Genome, and pathway networks. The most significant module based on protein-protein interaction (PPI) network was selected, and the genes in the module were identified as hub genes. Furthermore, survival analysis and translational level of hub genes were performed to verify the results.

Results: A total of 301 upregulated DEGs and 128 downregulated DEGs were identified. Pathways in cancer, focal adhesion and Wnt signaling were found to play critical roles. Ten hub genes were identified from PPI network analysis. Expression levels of two key genes, *COL1A1* and *VCAN*, were significantly associated with worse prognosis of patients with advanced ovarian cancer.

Conclusions: Our findings suggest that pathways in cancer, focal adhesion, Wnt signaling, and expression levels of two key genes, *COL1A1* and *VCAN*, may become novel targets for the diagnosis and therapy of ovarian cancer with omental metastasis.

Keywords: Ovarian cancer; Omental metastasis; Differentially expressed genes; GSE120196; Bioinformatics analysis; Hub genes.

Abbreviations: OC, ovarian cancer; HGSOC, high-grade serous ovarian cancer; DEGs, differentially expressed genes; GO, gene ontology; KEGG, Kyoto Encyclopedia of Genes and Genomes; PPI network, protein-protein interaction network; GCBI, Gene-Cloud of Biotechnology Information; GEO, Gene Expression Omnibus; NCBI, National Centre of Biotechnology Information; *GPM6A*, *glycoprotein M6A*; *SERPINE2*, *serpin peptidase inhibitor*, *clade E*, *member 2*; *COL1A1*, *collagen type I alpha 1*; *TM4SF1*, *transmembrane 4L six family member 1*; *TP53*, *tumor protein p53*; *HSPD1*, *heat shock protein family D (Hsp60) member 1*; *CSF3*, *colony stimulating factor 3*; *MARS*, *methionyl-tRNA synthetase*; *F2R*, *coagulation factor II (thrombin) receptor*; *VCAN*, *versican*; *C2orf40*, *chromosome 2 open reading frame 40*; *SLC24A3*, *solute carrier family 24 member 3*; *EIF1*, *eukaryotic translation initiation factor 1*; *GLYAT*, *glycine-N-acyltransferase*; *UGGT2*, *UDP-glucose glycoprotein glucosyltransferase 2*; *KANK4*, *KN motif and ankyrin repeat domains 4*; STRING, Search Tool for the Retrieval of Interacting Genes.

[*]**Correspondence to:** Jindian Tan, Department of Orthopaedic Surgery, Hainan General Hospital, Hainan Affiliated Hospital of Hainan Medical University, Haikou, China. ORCID: https://orcid.org/0000-0002-6185-3758. Tel: +86 0898-68622210, E-mail: tjd3108@163.com; Lin Wang; Department of Medical Oncology, Hainan General Hospital, Hainan Affiliated Hospital of Hainan Medical University, Haikou, China. ORCID: https://orcid.org/0000-0002-4003-784X. Tel: +86 0898-68642120, E-mail: wanglin7209@163.com

How to cite this article: Zhou M, Sheng L, Wang H, Zhang X, Tan J, Wang L. Identification of Omentum-derived Molecular Determinants and Pathways Mediating the Omental Metastasis of Ovarian Cancer. *Explor Res Hypothesis Med* 2022;7(4):228–240. doi: 10.14218/ERHM.2021.00048.

Introduction

Ovarian cancer (OC) is the seventh-most common malignancy in women worldwide, with the eighth-highest rate of cancer mortality, seriously threatening women's lives.[1,2] The most common subtype of OC is serous ovarian cancer. Due to its anatomic location and the silent progression of OC, approximately 80% of patients

with OC are diagnosed at an advanced stage with an extremely poor prognosis.[3,4] Widespread pelvic and abdominal metastasis and planting is a major risk of death with OC.[5]

Ovarian cancer has a tendency to metastasize to the omentum, which is rich in adipocytes.[6] Omental metastasis of OC is closely associated with the metastatic progression of the tumor.[7] At present, it is not clear why ovarian cancer cells preferentially metastasize to and proliferate in the omentum. Studies have revealed that OC preferentially seeds in the omental fat band, not merely because of the anatomical structure of the omentum, but also partially because a series of changes occur at the transcriptional level in adipocytes in the omentum, induced by the cancer microenvironment, that promote homing and omental metastasis of ovarian cancer cells.[8] Furthermore, Nieman *et al*. found that lipid could directly transfer from adipocytes to ovarian cancer cells under co-culture conditions, promoting tumor growth *in vitro* and *in vivo*.[9] In addition, they demonstrated that co-culture of adipocyte-ovarian cancer cells induces fat metabolism and β-oxidation in cancer cells, indicating that adipocytes serve as energy sources for cancer cells.

After migrating to the omentum, ovarian cancer cells grow much faster than primary tumor cells, suggesting that the omentum can facilitate tumor cells to migrate, colonize, invade new sites, and proliferate.[9] However, research has not yet elucidated specific omentum-derived molecular factors that regulate OC progression. Gene chip technology has recently undergone rapid development, and has become widely used due to its advantages of efficiency, large-scale implementation and high throughput capabilities. At present, gene chip technology has been widely adopted to assist with the discovery of biomarkers for early diagnosis and molecular typing of ovarian tumors and for establishing prognostic models.[10–12] Using bioinformatic analyses to explore the mechanisms involved in the omental metastasis of OC could facilitate the clinical management of this disease.

Herein, in order to identify genes that may be involved in the omental metastasis of OC, we used the gene expression profile GSE120196 dataset from the Gene Expression Omnibus (GEO) database to search for genes that are differentially expressed in omental adipose tissues from patients with benign gynecologic disease and patients with OC. This included performing gene ontology (GO), Kyoto Encyclopedia of Genes and Genome (KEGG), and PPI-network analyses to identify hub genes and key genes that may play significant mechanistic roles in the omental metastasis of OC and form possible therapeutic targets.

Materials and methods

Gene-Cloud of Biotechnology Information (GCBI)

GCBI (https://www.gcbi.com.cn) is an R-based online comprehensive analysis software suite developed in Shanghai, China, which integrates genetic information, sample information, research findings, data algorithms and bioinformatics. The GCBI platform includes data from 120 million copies of genomic samples, as well as approximately 90,000 copies of tumor samples and as many as 17 million copies of genetic information.[13–15] In the current study, we used the GCBI platform to identify DEGs between OC and normal control (NC; the omental tissues from four patients with benign gynecologic diseases). The DEGs were then used for GO enrichment analysis, KEGG analysis, pathway network analysis, and PPI network analysis.

Gene Expression Omnibus (GEO) DataSets

The GEO DataSets (http://www.ncbi.nlm.nih.gov/gds) at National Centre of Biotechnology Information (NCBI) form the largest and most comprehensive public functional collection of genomic datasets.[16] The key words "omental adipose tissue of ovarian cancer" were used to search GEO datasets and the gene chip dataset GSE120196. The GSE120196 dataset was obtained based on the GPL570 platform [HG-U133_Plus_2], with Affymetrix Human Genome U133 Plus 2.0 Array included for the subsequent analysis. The GSE120196 dataset contains a total of 14 samples, including 10 cancer-associated omental adipose tissues obtained from high-grade serous OC (HGSOC) patients and 4 micro-dissected omental adipose tissue samples from patients with benign gynecologic diseases.

Identification of DEGs

The GCBI laboratory provides seven function modules, including sample grouping, differential gene expression analysis, GO enrichment analysis, KEGG pathway analysis, and network analysis.[17] The information from the GeneChip Sample was entered into the GCBI online laboratory (https://www.gcbi.com.cn/gclib/html/index) to identify DEGs and conduct subsequent analyses. Thresholds of $Q < 0.05$, $p < 0.05$ and log2 (fold change) > 1.2 were applied to filter and select DEGs between OC and NC samples.

GO enrichment analysis and pathway analysis

Based on the DEGs, GO enrichment analysis and pathway analysis using the GCBI online platform were performed using thresholds of $p < 0.05$ and false discovery rate (FDR) < 0.05 to reveal the biological functions of DEGs.[18] Pathway analysis was conducted using KEGG enrichment analysis with, the *p*-value for identifying metabolic processes set at $p < 0.05$. Furthermore, pathway network analysis was constructed to identify pathway connections and core networks using the GCBI platform. By assessing the upstream and downstream relationship between pathways, a deeper and broader understanding of signaling pathways can be established.

Protein-protein interaction (PPI) network and hub gene selection

Search Tool for the Retrieval of Interacting Genes (STRING) is a database of known and predicted protein-protein interactions. In this study, protein interaction networks were constructed using STRING version 11.0 online software (www.string-db.org/).[19] The top 100 DEGs were then mapped to STRING, and the interactions with a combined score of > 0.4 for PPI pairs were selected for construction of a PPI network using Cytoscape version 3.8.0 software. Hub genes and subnetworks were identified through network analysis using the cytoHubba plugin from Cytoscape v3.8.0.[20] The betweenness centrality values of the top 10 nodes in the networks were computed and were generated. Genes in this module were regarded as hub genes.

Statistical analysis

Kaplan-Meier survival analysis

Survival was analyzed using Kaplan-Meier survival analysis (https://kmplot.com/analysis/). Prognostic analysis was performed for progression free survival (PFS) or overall survival (OS). The following retrieval indexes were used: Gene symbol 'use multiple

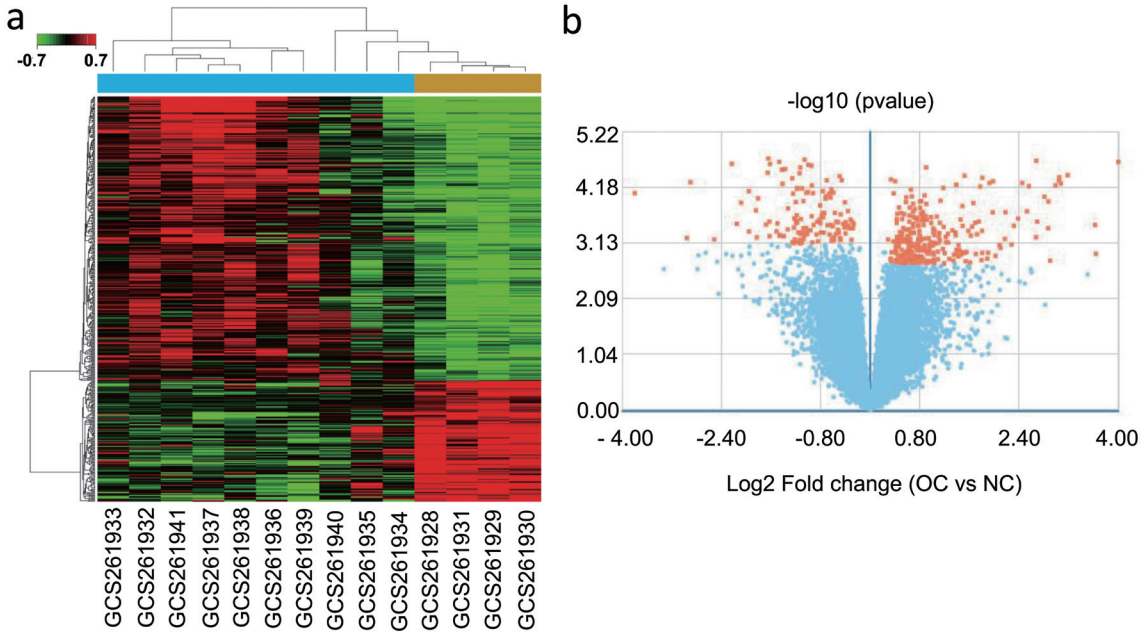

Fig. 1. Volcano plot and heat map of differentially expressed mRNAs. (a) Cluster heat map of the differentially expressed genes between OC and NC. The column represents tissue samples (OC blue; NC yellow) and the rows represent genes (red indicates higher gene expression; green indicates lower expression). (b) The volcano map of differential gene expression between OC and NC. OC and NC (normal control) represent cancer-associated adipose tissues from ovarian cancer patients and adipose tissues from patients with benign gynecologic diseases, respectively. Orange represents DEGs; the significantly up-regulated genes are plotted in orange on the right side and down-regulated genes plotted in orange on the left.

genes' field: enter top 10 hub gene name; split patients by: Upper Tertile; Stage: 3+4 stage; Survival: PFS or OS respectively. A *p*-value <0.01 was considered statistically significant.

Oncomine analysis

The Oncomine database (http://www.oncomine.org) is a cancer gene chip database and integrated data-mining platform. It includes gene information covering 33 different cancers and can be used to analyze the differential expression of genes between cancer and adjacent normal tissue. In this study, the mRNA expression levels of *COL1A1*, *VCAN*, and *MARS* in ovarian cancer tissues and normal tissues were acquired. The settings were as follows: Gene: *COL1A1*, *VCAN*, and *MARS*, respectively; Analysis Type: Cancer vs Normal analysis; Cancer type: Ovarian cancer; Sample type: Clinical specimen; Data type: mRNA; Threshold (p-value < 0.001, fold change > 1.5, gene rank = top 10%).

Results

Identification of differentially expressed genes (DEGs)

To identify DEGs in omental adipose tissues from ovarian cancer patients, the transcription profile dataset GSE120196 was obtained from the NCBI GEO database, which includes information from 10 patients with HGSOC and 4 patients with benign gynecologic diseases as controls. Thresholds were set at Q < 0.05, p < 0.05 and log2 (fold change) > 1.2 for differential expression analysis. A total of 429 DEGs were identified, which included 301 genes that were significantly up-regulated and 128 genes that were significantly down-regulated. These results were visualized as a heat map and a volcano plot (Fig. 1). The top 12 genes displaying the most significant changes in expression were unnamed, *glycoprotein M6A (GPM6A)*, *serpin peptidase inhibitor*, *clade E, member 2 (SERPINE2)*, *collagen type I alpha 1 (COL1A1)*, *transmembrane 4L six family member 1(TM4SF1)* , *chromosome 2 open reading frame 40 (C2orf40)*, *unnamed, solute carrier family 24 member 3 (SLC24A3)*, *eukaryotic translation initiation factor 1(EIF1)*, *glycine-N-acyltransferase (GLYAT)*, *UDP-glucose glycoprotein glucosyltransferase 2 (UGGT2)*, *and KN motif and ankyrin repeat domains 4 (KANK4)* (Table 1).

GO enrichment analysis of DEGs

To better understand the biological functions of these DEGs, GO enrichment analysis was performed using the platform of Gene-Cloud of Biotechnology Information (GCBI) for all DEGs. GO analysis was conducted based on Fisher exact test. Using statistical difference thresholds of p < 0.05 and FDR < 0.05, we identified 145 sequences potentially involved in biological processes. The most common biological processes identified were negative regulation of cell proliferation, extracellular matrix organization, positive regulation of cell proliferation, collagen fibril organization, negative regulation of apoptotic process, collagen catabolic process, extracellular matrix disassembly, cell adhesion, skeletal system development, positive regulation of ERK1 and ERK2 cascade (Table 2 and Fig. 2a).

KEGG pathway enrichment analysis of DEGs

KEGG is a powerful tool for the analysis of metabolic pathways and networks. The GCBI platform-based KEGG pathway enrichment analysis of DEGs showed that DEGs were enriched in 43

Table 1. The top 12 genes with the most significant differential expression

Gene symbol	Gene description	*p*-value	Gene feature	Rank
Unnamed	–	1.90E−05	down	1
GPM6A	*glycoprotein M6A*	2.00E−05	down	2
SERPINE2	*serpin peptidase inhibitor, clade E, member 2*	2.10E−05	up	3
COL1A1	*collagen, type I, alpha 1*	2.20E−05	up	4
TM4SF1	*transmembrane 4 L six family member 1*	2.20E−05	down	5
C2orf40	*chromosome 2 open reading frame 40*	2.40E−05	down	6
Unnamed	–	2.40E−05	down	7
SLC24A3	*solute carrier family 24, member 3*	2.50E−05	down	8
EIF1	*eukaryotic translation initiation factor 1*	2.60E−05	down	9
GLYAT	*glycine-N-acyltransferase*	2.80E−05	down	10
UGGT2	*UDP-glucose glycoprotein glucosyltransferase 2*	2.80E−05	up	11
KANK4	*KN motif and ankyrin repeat domains 4*	3.00E−05	down	12

pathways with a statistical significance of $p < 0.05$. The enriched pathways were mainly in categories such as "PI3K-Akt signaling" (p = 3.17E-10), "Cytokine-cytokine receptor interaction" (p = 3.09E−08), "Focal adhesion" (p = 9.09E−07), "ECM-receptor interaction" (p = 7.92E−06), "Protein digestion and absorption" (p = 8.55E−06), "Jak-STAT signaling" (p = 5.01E−05), "Malaria" (p = 6.23E−05), "Pathways in cancer" (p = 7.38E−05), "Protein processing in endoplasmic reticulum" (p = 7.44E−05), and "Transcriptional mis-regulation in cancer" (p = 1.26E−04). The top 20 enriched pathway terms are displayed in Figure 2b.

Pathway network analysis of significant pathways

Pathway network analysis was constructed based on the interaction relationships provided by the KEGG database. From this network,

Table 2. The top 20 significant GO terms for biological processes. FDR indicates false discovery rate

BP name	Enrichment score	*p*-value	FDR	Rank
Negative regulation of cell proliferation	7.94	8.82E−13	6.29E−10	1
Extracellular matrix organization	10.96	9.14E−13	6.29E−10	2
Positive regulation of cell proliferation	7.25	1.51E−12	6.90E−10	3
Collagen fibril organization	31.25	2.04E−11	7.02E−09	4
Negative regulation of apoptotic process	5.87	2.52E−10	6.89E−08	5
Collagen catabolic process	18.81	3.01E−10	6.89E−08	6
Extracellular matrix disassembly	17.14	7.72E−10	1.52E−07	7
Cell adhesion	5.67	3.53E−09	6.07E−07	8
Skeletal system development	11.73	6.26E−09	9.56E−07	9
Positive regulation of ERK1 and ERK2 cascade	14.01	3.62E−08	4.98E−06	10
Transforming growth factor beta receptor signaling pathway	11.19	5.16E−08	6.45E−06	11
Positive regulation of transcription, DNA-dependent	4.96	7.21E−08	8.26E−06	12
Negative regulation of cell growth	10.42	4.81E−07	5.08E−05	13
Negative regulation of platelet activation	60.18	7.15E−07	7.02E−05	14
Blood vessel development	20.83	8.24E−07	7.55E−05	15
Positive regulation of MAPK cascade	14.81	9.73E−07	8.36E−05	16
Positive regulation of protein kinase B signaling cascade	13.94	1.48E−06	1.20E−04	17
Chondroitin sulfate biosynthetic process	27.08	2.01E−06	1.53E−04	18
Cell-cell signaling	6.15	4.40E−06	3.19E−04	19
Platelet activation	6.64	6.54E−06	4.50E−04	20

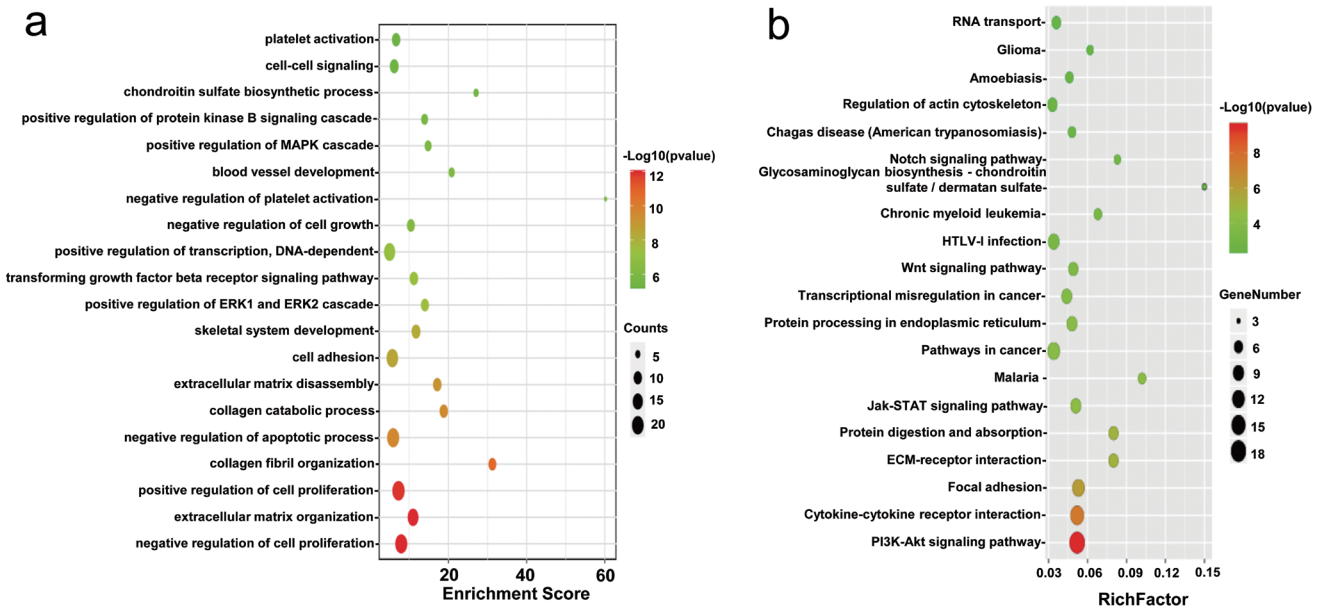

Fig. 2. GO and KEGG pathway enrichment analysis. (a) The top 20 enrichment scores in GO enrichment analysis of DEGs. (b) Analysis of the top 20 enriched KEGG pathways.

we analyzed signal transduction of the significant upstream regulatory signaling pathways and downstream effectors in order to better understand the nature of the differences between the samples. A total of 17 pathways were identified, of which 11 were up-regulated. Six differentially regulated pathways were significantly enriched. We identified 31 relationships between these pathways (Fig. 3). As shown in Table 3, the main signaling pathways implicated in cancer-associated omental tissue were: pathways in cancer, focal adhesion, Wnt signaling, TGF-beta signaling, and cytokine-cytokine receptor interaction. Pathways in cancer was the key node in this network with the most extensive interactions with the remaining pathways.

Construction of the PPI network and identification of hub genes

PPI network analysis constructs a network of protein interactions as well as identifying hub genes. The PPI network of the top 100 DEGs obtained from the GSE120196 dataset was constructed using the STRING database and Cytoscape software. This revealed a PPI network containing 43 hub nodes and 62 edges (Fig. 4a). The top 10 of these 43 genes were screened as hub genes using the betweenness method of the cytoHubba plugin. These genes included *TP53*, *COL1A1*, *HSPD1*, *SERPINE2*, *CSF3*, *MARS*, *F2R*, *VCAN*, *COL1A2*, and *THBD* (Table 4). The expanded subnetwork of the top 10 hub genes is shown in Figure 4b.

Kaplan-Meier analysis of hub genes

In the above analyses, we studied gene networks derived from OC with greater omentum metastases. To investigate the association between gene networks and OC further, we performed Kaplan-Meier survival analyses to investigate the association of ten hub genes with PFS and OS of advanced-stage ovarian cancer (FIGO Stage III–IV). We found that patients with higher expression levels of *COL1A1* or *VCAN* had significantly lower PFS rates, and patients with higher expression levels of *MARS* had longer PFS rates (Fig. 5a), with these differences being statistically significant ($p = 0.0022$, $p = 0.0025$, and $p = 0.00017$, respectively). Moreover, survival analysis showed that only *VCAN* expression was negatively correlated with overall survival (Fig. 5b, $p = 0.0031$). The expression levels of the remaining genes were not significantly associated with survival.

Validation of gene expression based on the Oncomine database

To further investigate mRNA expression levels of *COL1A1*, *VCAN* and *MARS* in ovarian cancer, our study used the Oncomine database. Results showed that *COL1A1*, *VCAN* and *MARS* mRNA expression levels were significantly higher in tumor samples than samples from non-cancerous tissues (see Figs. 6a, 7a, 8a). To further understand the expression of these genes in human ovarian cancer, their expression level in normal ovary vs. ovarian cancer tissues were compared. *COL1A1*, *VCAN* and *MARS* mRNA levels were significantly higher in ovarian cancer tissues than those in the adjacent normal tissues (Fig. 6b, $p = 1.99E{-}12$; Fig. 7b, $p = 2.88E{-}4$; Fig. 8b, $p = 1.02E{-}4$), and were each highly expressed in different histological types of human ovarian cancer (all $p < 0.001$; Fig. 6c, Fig. 7c and Fig. 8c).

In summary, survival analysis identified three up-regulated hub genes that were associated with survival. Increased *COL1A1* and *VCAN* expression correlated with poorer survival, while in contrast higher expression of *MARS* was associated with longer PFS. Since *COL1A1* and *VCAN* expression levels were significantly correlated with the prognosis of advanced OC patients, they may be useful as novel targets for diagnosis and therapy in OC patients with omental metastasis.

Discussion

Ovarian cancer metastasis is a complex process that involves numerous influential factors and multiple steps. The metastatic routes of OC principally consist of direct spread, intraperitoneal implan-

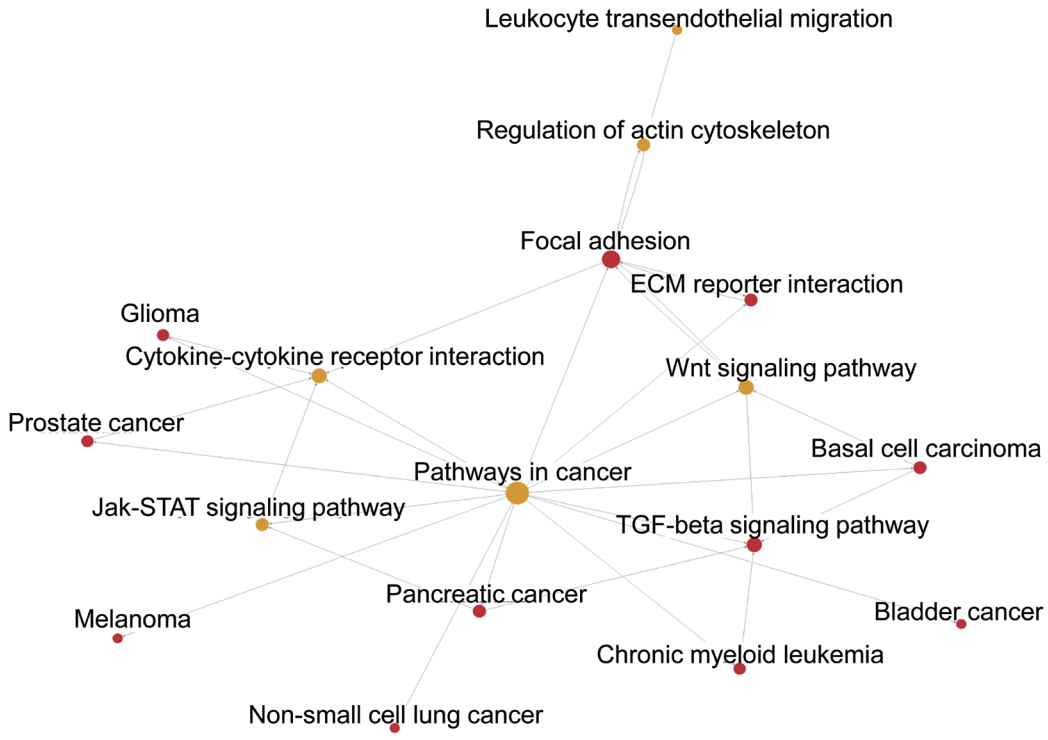

Fig. 3. The pathway interaction network. A node indicates a pathway, and the size of the node represents the value of the degree (the larger the node, the greater the degree). Expression levels are represented in different colors (red: up-regulation; yellow: both up- and down-regulation; blue: down-regulation).

tation metastasis and lymphatic metastasis. Hematogenous metastasis only occurs rarely.[9,21] Exfoliated tumor cells from advanced OC are widely disseminated in the abdominal-pelvic cavity, and the greater omentum is the most common metastatic site of ovarian cancer.[7] The greater omentum is an important immune organ in the abdominopelvic cavity, which covers the surface of the viscera and is richly supplied with blood vessels, lymphatic drainage, adipose tissue, and nerve fibers. It also is known to have anti-tumor properties. However, in advanced ovarian cancer the greater omentum is often contracted into a pie shape due to extensive seeding of tumor cells. Dynamic observation of animal models of ovarian tumors conducted at the University of Chicago showed that ovarian cancer cells infiltrate the greater omentum within 20 minutes of entering the abdominal cavity.[22] Therefore, the study of omental metastasis in ovarian cancer has become an important focus of research in recent years. Nowicka isolated pluripotential adipose-derived stem cells from ovarian cancer patients' greater omentum, indicating that adipose-derived stem cells could promote the proliferation and migration of tumor cells and contribute to their resistance to chemotherapy.[23] Additionally, previous studies have shown that ovarian cancer cells can induce lipolysis in the omentum, which can provide energy for the invasion and metastasis of tumor cells.[9] Despite progress in studying on omental metastasis of OC, the underlying mechanisms are still not fully elucidated.

Table 3. The 10 highest scoring pathway in pathway network analysis

Pathway name	Outdegree	Indegree	Degree	Pathway feature
Pathways in cancer	14	0	14	up|down
Focal adhesion	4	4	8	up
Wnt signaling pathway	2	3	5	up|down
TGF-beta signaling pathway	0	5	5	up
Cytokine-cytokine receptor interaction	0	5	5	down|up
ECM-receptor interaction	1	2	3	up
Jak-STAT signaling pathway	1	2	3	down|up
Regulation of actin cytoskeleton	1	2	3	down|up
Pancreatic cancer	2	1	3	up
Basal cell carcinoma	2	1	3	up

Higher degree values indicate pathways with more importance role in the signaling network.

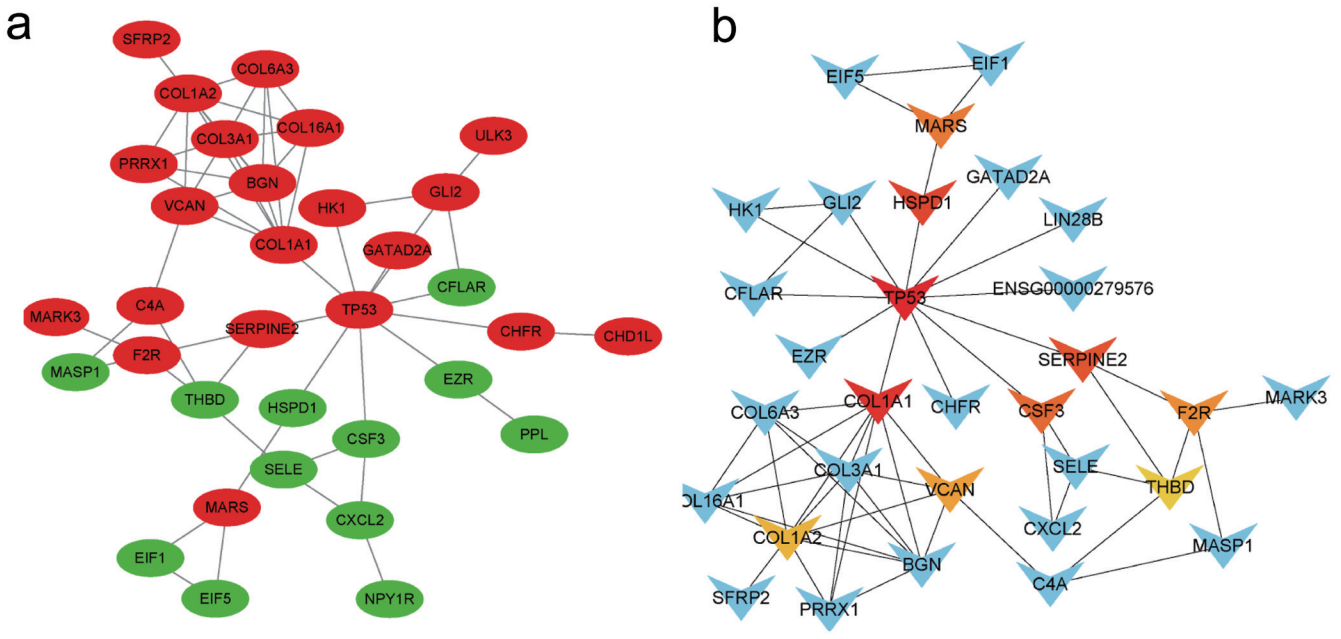

Fig. 4. PPI network and hub genes. (a) The PPI network of top 100 DEGs with a minimum interaction score of 0.4 were visualized in Cytoscape software. Red represents up-regulated genes; green represents down-regulated genes. (b) The PPI network of the top 10 hub genes. Hub genes are presented in color depth of red to yellow, with other interaction genes shown in blue. The color depth represents the betweenness value (the redder the dot, the more important the hub gene).

Gene chip technology makes it possible to explore specific mechanisms of ovarian cancer occurrence at the genomic level and then focus more precisely on the identified gene targets. In this study, we sought to explore and analyze the gene chip detection data of RNA samples from cancer-associated omental tissues derived from ten patients with OC and benign control tissues derived from four patients in order to identify differentially expressed genes related to the omental metastasis of OC. Our findings show significant differences in the gene expression profiles of the two sets of tissues. Among more than 50,000 genes detected, a total of 429 genes are differentially expressed, including 301 up-regulated genes and 128 down-regulated genes, potentially identifying genes affecting tumor development. We further screened the top 12 genes identified by these analyses (unnamed, *GPM6A*, *SERPINE2*, *COL1A1*, *TM4SF1*, *C2orf40*, unnamed, *SLC24A3*, *EIF1*, *GLYAT*, *UGGT2*, and *KANK4*). Of special note, expression of *GPM6A* was the lowest.

GO analysis revealed that differentially expressed genes have functions that are mainly related to cell proliferation, extracellular matrix, collagen, and cell adhesion. The PI3K-Akt signaling pathway, cytokine-cytokine receptor interaction, focal adhesion, ECM-receptor interaction, protein digestion and absorption, Jak-STAT signaling, and other pathways in cancer were also identified by KEGG pathway enrichment analysis. Prior research has shown that the progression of malignant tumors is often accompanied by changes in the construction of the extracellular matrix and expression of cell surface receptors,[24,25] consistent with our findings in cancer-associated omental tissues from the patients with advanced stage, high-grade serous ovarian cancer (HGSOC) in the current

Table 4. The top 10 hub genes were identified by cytoHubba

Gene symbol	Gene feature	Gene description	Betweenness
TP53	up	*tumor protein p53*	864.2
COL1A1	up	*collagen, type I, alpha 1*	368.23
HSPD1	down	*heat shock 60kDa protein 1 (chaperonin)*	186
SERPINE2	up	*serpin peptidase inhibitor, clade E (nexin, plasminogen activator inhibitor type 1), member 2*	170.2
CSF3	down	*colony stimulating factor 3 (granulocyte)*	144
MARS	up	*methionyl-tRNA synthetase*	128
F2R	up	*coagulation factor II (thrombin) receptor*	105.33
VCAN	up	*versican*	76.47
COL1A2	up	*collagen, type I, alpha 2*	72.7
THBD	down	*thrombomodulin*	69.67

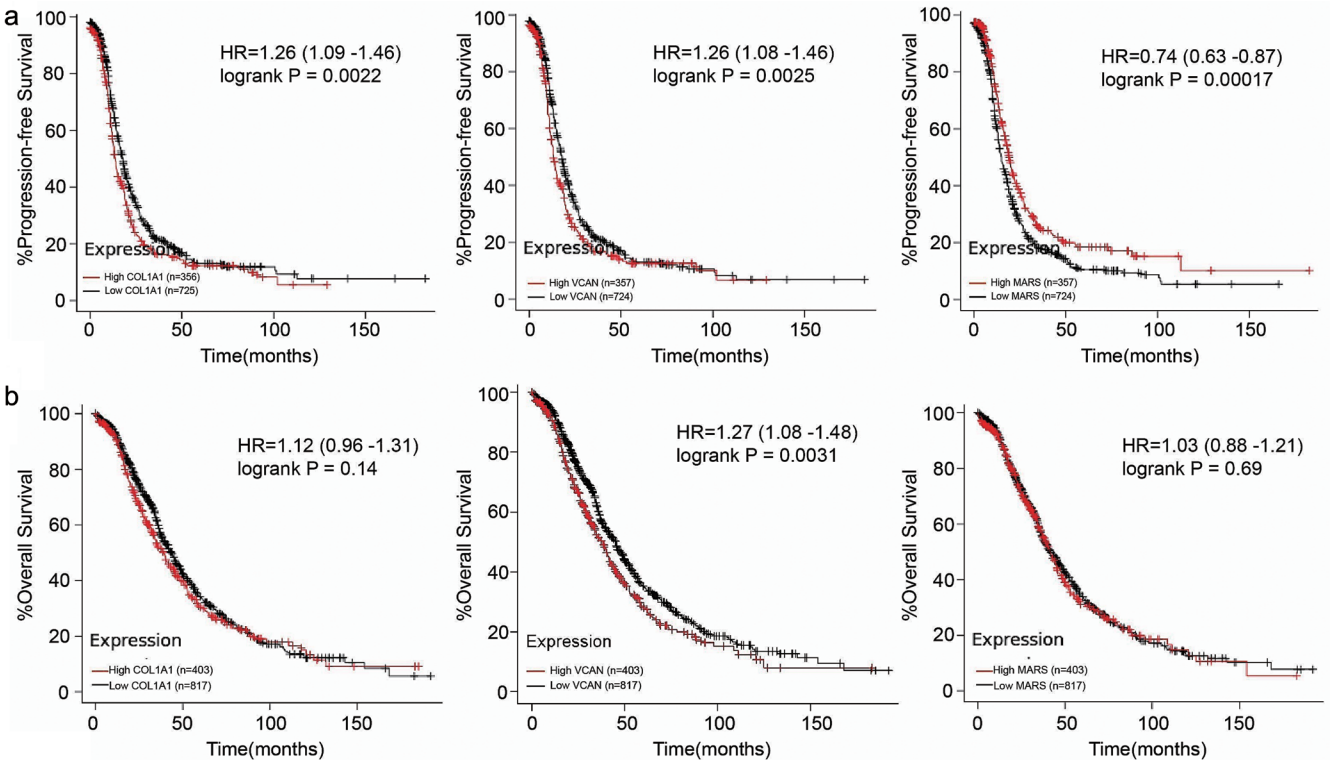

Fig. 5. Kaplan-Meier analysis of hub genes. (a) The relationship of *COL1A1*, *VCAN* and *MARS* expression with PFS in FIGO stage III–IV ovarian cancer; (b) The relationship of *VCAN* expression with OS in FIGO stage III–IV ovarian cancer.

study. In addition, changes in collagen content within tumor cells and the tumor microenvironment play an essential role in the invasion and metastasis of tumor cells by affecting tumor metabolism, gene expression, angiogenesis, and epithelial-mesenchymal transition.[26–30]

In the current study, we found that genes that were significantly differentially expressed were involved in 43 pathways, including PI3K-Akt signaling, cytokine-cytokine receptor interaction, focal adhesion, and ECM-receptor interaction. The activation of PI3K-AKT pathway is important for cancer cell proliferation, migration, invasion, and chemoresistance, including in ovarian cancer cells.[31,32] In the PPI network analysis, a total of ten hub genes formed the center of the network: *TP53*, *COL1A1*, *HSPD1*, *SERPINE2*, *CSF3*, *MARS*, *F2R*, *VCAN*, *COL1A2* and *THBD*. With the exception of *HSPD1*, *CSF3* and *THBD*, each of these genes were up-regulated in metastatic ovarian cancer-associated samples compared to samples from patients with benign gynecologic diseases.

The present study implicated several DEGs in the development and progression of ovarian cancer, including *COL1A1*, *VCAN*, and *MARS*. In addition, examination of the association between expression levels of ten hub genes and patients' PFS and OS demonstrated that higher expression levels of *VCAN* were associated with worse PFS and OS, higher expression levels of *COL1A1* were associated with reduced PFS, and that higher expression of *MARS* correlated with increased PFS. These findings on *MARS* are not consistent with previous studies in which *MARS* expression is up-regulated and positively correlated with poor prognosis in various cancers, such as breast cancer and lung cancer. Taken together, we conclude that *MARS* may not be a regulator for advanced ovarian cancer. *COL1A1* and *VCAN*, which were identified as key genes associated with OC survival in the current study, could be useful as diagnostic and prognostic biomarkers.

Studies have suggested that aberrant expression of *COL1A1* is closely related to tumorigenesis in several malignancies.[33–36] *COL1A1* expression can induce the epithelial-mesenchymal transition, thus promoting invasion and metastasis of tumor cells.[37] Liu *et al*. confirmed that *COL1A1* is a potential therapeutic target for breast cancer as it mediates the metastatic process.[38] Recent studies have suggested that *COL1A1* may be a biomarker for early detection of gastric cancer.[39] Moreover, up-regulation of *COL1A1* may contribute to cisplatin resistance in ovarian cancer cells.[40] Our results show that *COL1A1* expression was significantly up-regulated in OC-associated omental tissues. In addition, patients with higher *COL1A1* expression had worse PFS.

VCAN belongs to the family of large aggregating chondroitin sulfate proteoglycans and is mainly found in the extracellular matrix.[41] *VCAN* expression levels have been shown to correlate with tumor progression, and are a poor prognostic indicator in stage II–III colon cancer patients.[42] Kulbe *et al*. have suggested that *VCAN* has the potential to be used as a biomarker for ovarian cancer,[43] as stromal *VCAN* is a biomarker with a poor prognosis.[44] Our study showed that high *VCAN* expression is associated with worse PFS and OS in patients with advanced OC, suggesting that it may be implicated in the omental metastasis of OC.

Future directions

Herein, we identified two key genes, *COL1A1* and *VCAN*, which may play a key role in the omental metastasis of OC. These genes may be useful as new prognostic biomarkers for advanced OC. Further studies are needed to validate the roles played by *COL1A1*

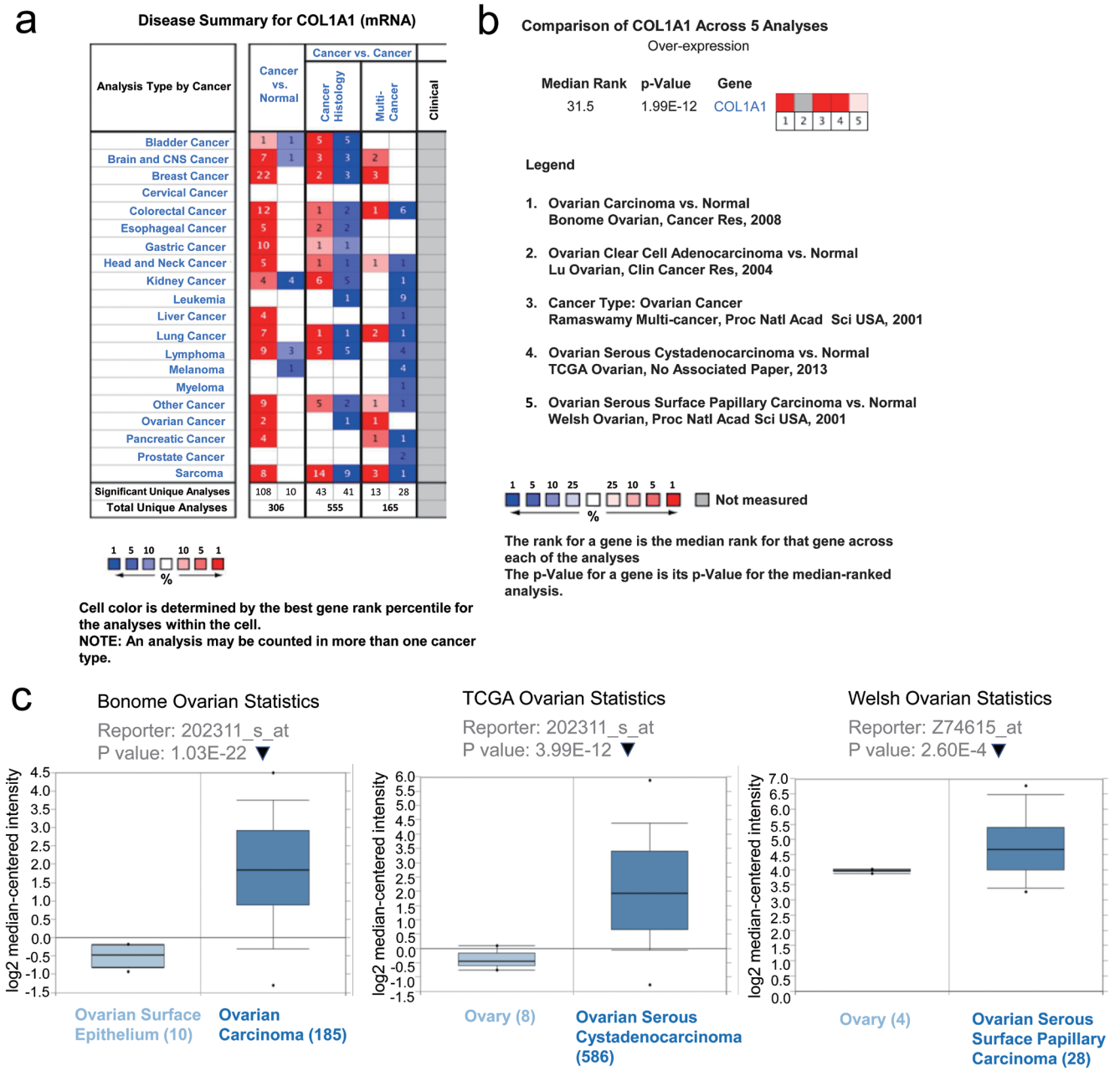

Fig. 6. Validation of *COL1A1* gene expression based on the Oncomine database. (a) Summarization of *COL1A1* expression in various cancer types from the Oncomine database. Red denotes significant overexpression; (b) Expression of *COL1A1* mRNA levels in human ovarian cancers using the Oncomine database; (c) Expression levels of *COL1A1* in different ovarian cancer datasets.

and *VCAN genes* in advanced OC and their role in the progression of early stages of OC.

Conclusions

This study used comprehensive bioinformatics to identify two genes (*COL1A1* and *VCAN*), which may serve key roles in the tumorigenesis of OC with omental metastasis (Fig. 9). These key genes could serve as novel prognostic biomarkers of advanced OC. However, a limitation of the current study is the lack of *in vivo* and *in vitro* experiments. Further experiments are required to confirm the present findings, and explore the specific mechanisms and the exact functions of these genes in advanced-stage OC.

Acknowledgments

We are grateful to researchers who have deposited their data in the GEO database. The authors would like to acknowledge the techni-

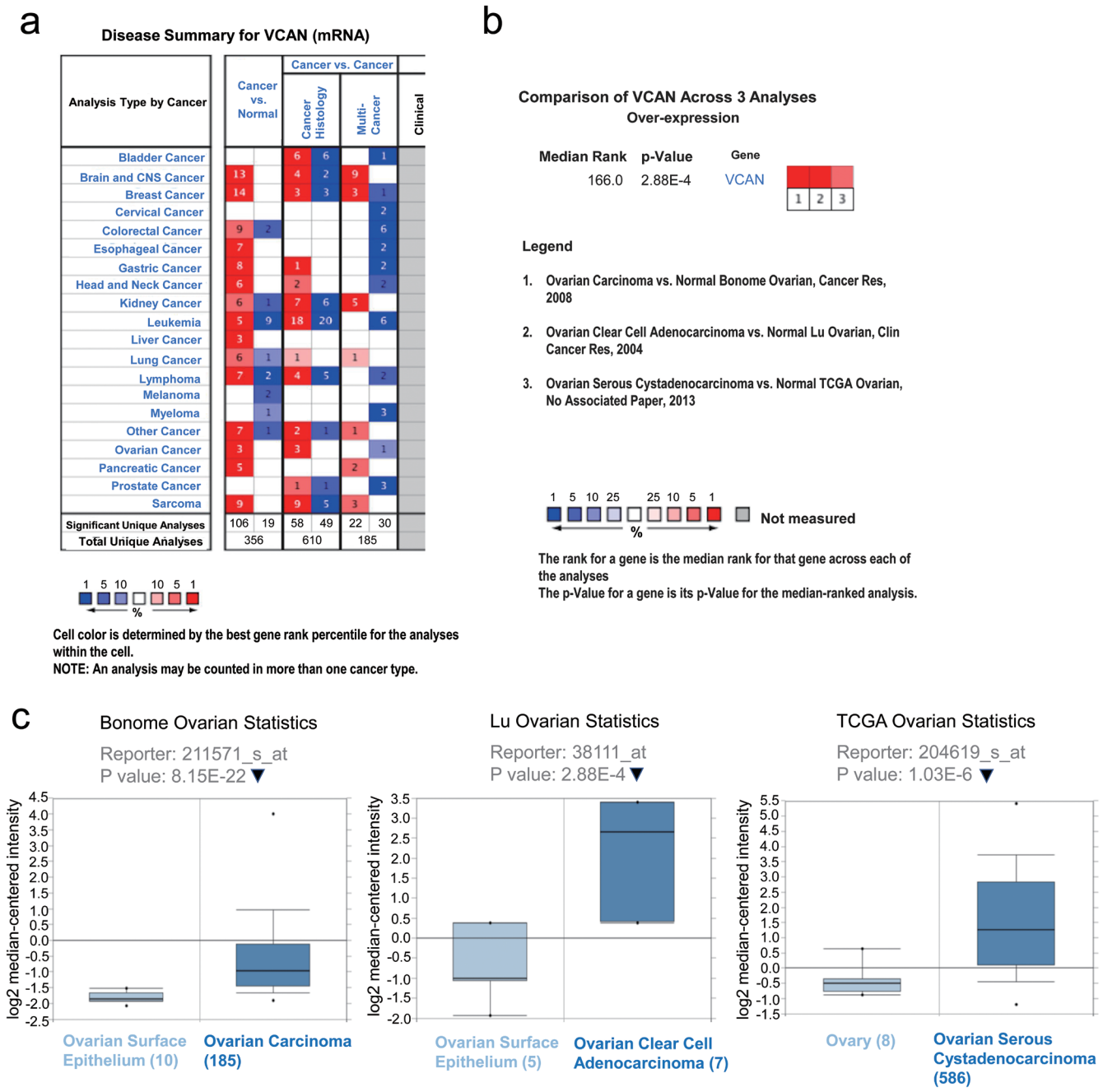

Fig. 7. Validation of *VCAN* gene expression based on the Oncomine database. (a) Summary of *VCAN* expression in various cancer types from the Oncomine database. Red denotes significant overexpression; (b) Expression of *VCAN* mRNA levels in human ovarian cancers using the Oncomine database; (c) Expression levels of *VCAN* in different ovarian cancer datasets.

cal assistance of the GCBI online analysis platform.

Funding

This work was supported by grants from Hainan health science and education project [Item No. 21A200020] and Hainan health science and education project [Item No. 20A200415].

Conflict of interest

The authors declare no competing interests.

Author contributions

MZ and LW conceived and designed the project; MZ and JT per-

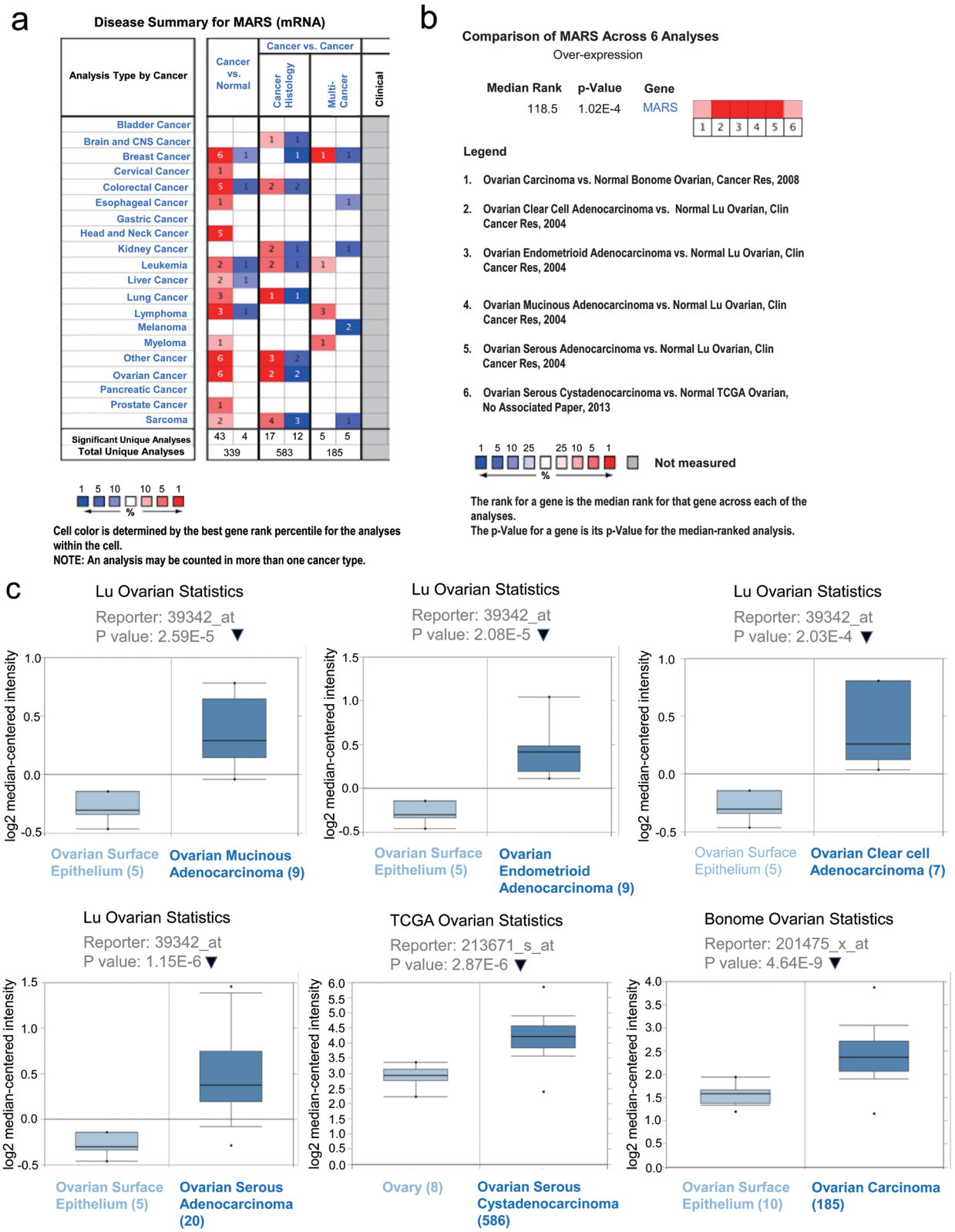

Fig. 8. Validation of *MARS* gene expression based on the Oncomine database. (a) Summary of *MARS* expression in various cancer types from the Oncomine database. Red denotes significant overexpression; (b) Expression of *MARS* mRNA levels in human ovarian cancers using the Oncomine database; (c) Expression levels of *MARS* in different ovarian cancer datasets.

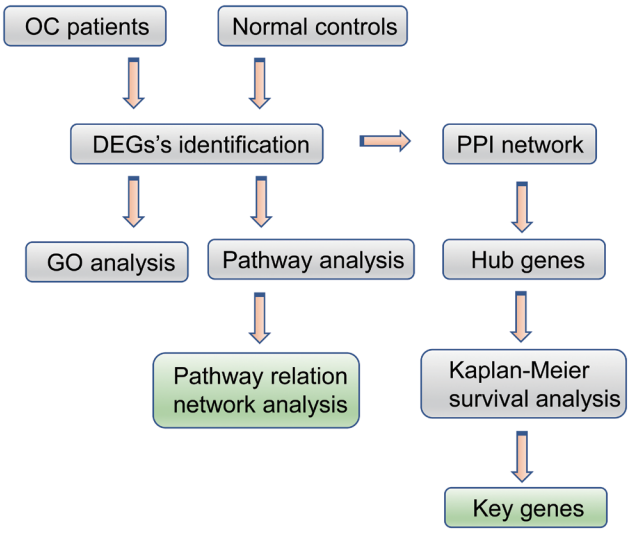

Fig. 9. Schematic summary of the present study.

formed the analysis and constructed the model; LS, HW and XZ checked the associated database and classified raw data; MZ and JT wrote and revised the manuscript. All of the authors read and approved the final manuscript.

Data sharing statement

The datasets generated and/or analyzed in the present study are available in the GEO (http://www.ncbi.nlm.nih.gov/gds) and the Oncomine (http://www.oncomine.org) repositories.

References

[1] Gaona-Luviano P, Medina-Gaona LA, Magaña-Pérez K. Epidemiology of ovarian cancer. Chin Clin Oncol 2020;9(4):47. doi:10.21037/cco-20-34, PMID:32648448.
[2] El-Sherif A, El-Sherif S, Taylor AH, Ayakannu T. Ovarian Cancer: Lifestyle, Diet and Nutrition. Nutr Cancer 2021;73(7):1092–1107. doi:10.1080/01635581.2020.1792948, PMID:32674720.
[3] Asante DB, Calapre L, Ziman M, Meniawy TM, Gray ES. Liquid biopsy in ovarian cancer using circulating tumor DNA and cells: Ready for prime time? Cancer Lett 2020;468:59–71. doi:10.1016/j.canlet.2019.10.014, PMID:31610267.
[4] Huang H, Liu N, Liao Y, Liu N, Cai J, Xia X, *et al*. Platinum-containing compound platinum pyrithione suppresses ovarian tumor proliferation through proteasome inhibition. J Exp Clin Cancer Res 2017;36(1):79. doi:10.1186/s13046-017-0547-8, PMID:28619062.
[5] Lengyel E. Ovarian cancer development and metastasis. Am J Pathol 2010;177(3):1053–1064. doi:10.2353/ajpath.2010.100105, PMID:20651229.
[6] Herrera CA, Xu L, Bucana CD, Silva EV, Hess KR, Gershenson DM, *et al*. Expression of metastasis-related genes in human epithelial ovarian tumors. Int J Oncol 2002;20(1):5–13. doi:10.3892/ijo.20.1.5, PMID:11743636.
[7] Naora H, Montell DJ. Ovarian cancer metastasis: integrating insights from disparate model organisms. Nat Rev Cancer 2005;5(5):355–366. doi:10.1038/nrc1611, PMID:15864277.
[8] Wang E, Ngalame Y, Panelli MC, Nguyen-Jackson H, Deavers M, Mueller P, *et al*. Peritoneal and subperitoneal stroma may facilitate regional spread of ovarian cancer. Clin Cancer Res 2005;11(1):113–122. PMID:15671535.
[9] Nieman KM, Kenny HA, Penicka CV, Ladanyi A, Buell-Gutbrod R, Zillhardt MR, *et al*. Adipocytes promote ovarian cancer metastasis and provide energy for rapid tumor growth. Nat Med 2011;17(11):1498–1503. doi:10.1038/nm.2492, PMID:22037646.
[10] Lu KH, Patterson AP, Wang L, Marquez RT, Atkinson EN, Baggerly KA, *et al*. Selection of potential markers for epithelial ovarian cancer with gene expression arrays and recursive descent partition analysis. Clin Cancer Res 2004;10(10):3291–3300. doi:10.1158/1078-0432.CCR-03-0409, PMID:15161682.
[11] Tothill RW, Tinker AV, George J, Brown R, Fox SB, Lade S, *et al*. Novel molecular subtypes of serous and endometrioid ovarian cancer linked to clinical outcome. Clin Cancer Res 2008;14(16):5198–5208. doi:10.1158/1078-0432.CCR-08-0196, PMID:18698038.
[12] Berchuck A, Iversen ES, Luo J, Clarke JP, Horne H, Levine DA, *et al*. Microarray analysis of early stage serous ovarian cancers shows profiles predictive of favorable outcome. Clin Cancer Res 2009;15(7):2448–2455. doi:10.1158/1078-0432.CCR-08-2430, PMID:19318476.
[13] Zhou T, Wang Y, Qian D, Liang Q, Wang B. Over-expression of TOP2A as a prognostic biomarker in patients with glioma. Int J Clin Exp Pathol 2018;11(3):1228–1237. PMID:31938217.
[14] Yang Z, Xu S, Jin P, Yang X, Li X, Wan D, *et al*. MARCKS contributes to stromal cancer-associated fibroblast activation and facilitates ovarian cancer metastasis. Oncotarget 2016;7(25):37649–37663. doi:10.18632/oncotarget.8726, PMID:27081703.
[15] Jiang YZ, Liu YR, Xu XE, Jin X, Hu X, Yu KD, *et al*. Transcriptome Analysis of Triple-Negative Breast Cancer Reveals an Integrated mRNA-lncRNA Signature with Predictive and Prognostic Value. Cancer Res 2016;76(8):2105–2114. doi:10.1158/0008-5472.CAN-15-3284, PMID:26921339.
[16] Xiao J, Liu A, Lu X, Chen X, Li W, He S, *et al*. Prognostic significance of TCF21 mRNA expression in patients with lung adenocarcinoma. Sci Rep 2017;7(1):2027. doi:10.1038/s41598-017-02290-2, PMID:28515486.
[17] Wang J, Yuan L, Liu X, Wang G, Zhu Y, Qian K, *et al*. Bioinformatics and functional analyses of key genes and pathways in human clear cell renal cell carcinoma. Oncol Lett 2018;15(6):9133–9141. doi:10.3892/ol.2018.8473, PMID:29805645.
[18] Liu Y, Xin ZZ, Zhang DZ, Wang ZF, Zhu XY, Tang BP, *et al*. Transcriptome analysis of yellow catfish (Pelteobagrus fulvidraco) liver challenged with polyriboinosinic polyribocytidylic acid (poly I:C). Fish Shellfish Immunol 2017;68:395–403. doi:0.1016/j.fsi.2017.07.030, PMID:28732769.
[19] Szklarczyk D, Franceschini A, Kuhn M, Simonovic M, Roth A, Minguez P, *et al*. The STRING database in 2011: functional interaction networks of proteins, globally integrated and scored. Nucleic Acids Res 2011;39(Database issue):D561–D568. doi:10.1093/nar/gkq973, PMID:21045058.
[20] Shannon P, Markiel A, Ozier O, Baliga NS, Wang JT, Ramage D, *et al*. Cytoscape: a software environment for integrated models of biomolecular interaction networks. Genome Res 2003;13(11):2498–2504. doi:10.1101/gr.1239303, PMID:14597658.
[21] Kenny HA, Dogan S, Zillhardt M, K Mitra A, Yamada SD, Krausz T, *et al*. Organotypic models of metastasis: A three-dimensional culture mimicking the human peritoneum and omentum for the study of the early steps of ovarian cancer metastasis. Cancer Treat Res 2009;149:335–351. doi:10.1007/978-0-387-98094-2_16, PMID:19763444.
[22] Lee D, Wada K, Taniguchi Y, Al-Shareef H, Masuda T, Usami Y, *et al*. Expression of fatty acid binding protein 4 is involved in the cell growth of oral squamous cell carcinoma. Oncol Rep 2014;31(3):1116–1120. doi:10.3892/or.2014.2975, PMID:24425381.
[23] Nowicka A, Marini FC, Solley TN, Elizondo PB, Zhang Y, Sharp HJ, *et al*. Human omental-derived adipose stem cells increase ovarian cancer proliferation, migration, and chemoresistance. PLoS One 2013;8(12):e81859. doi:10.1371/journal.pone.0081859, PMID:24312594.
[24] Kojima M, Higuchi Y, Yokota M, Ishii G, Saito N, Aoyagi K, *et al*. Human subperitoneal fibroblast and cancer cell interaction creates microenvironment that enhances tumor progression and metastasis. PLoS One 2014;9(2):e88018. doi:10.1371/journal.pone.0088018, PMID:24505356.
[25] Hynes RO. The extracellular matrix: not just pretty fibrils. Science 2009;326(5957):1216–1219. doi:10.1126/science.1176009, PMID:19965464.

[26] Morris BA, Burkel B, Ponik SM, Fan J, Condeelis JS, Aguirre-Ghiso JA, *et al*. Collagen Matrix Density Drives the Metabolic Shift in Breast Cancer Cells. EBioMedicine 2016;13:146–156. doi:10.1016/j.ebiom.2016.10.012, PMID:27743905.
[27] Esbona K, Inman D, Saha S, Jeffery J, Schedin P, Wilke L, *et al*. COX-2 modulates mammary tumor progression in response to collagen density. Breast Cancer Res 2016;18(1):35. doi:10.1186/s13058-016-0695-3, PMID:27000374.
[28] Huijbers IJ, Iravani M, Popov S, Robertson D, Al-Sarraj S, Jones C, *et al*. A role for fibrillar collagen deposition and the collagen internalization receptor endo180 in glioma invasion. PLoS One 2010;5(3):e9808. doi:10.1371/journal.pone.0009808, PMID:20339555.
[29] Maragoudakis ME, Missirlis E, Karakiulakis GD, Sarmonica M, Bastakis M, Tsopanoglou N. Basement membrane biosynthesis as a target for developing inhibitors of angiogenesis with anti-tumor properties. Kidney Int 1993;43(1):147–150. doi:10.1038/ki.1993.24, PMID:7679456.
[30] Vellinga TT, den Uil S, Rinkes IH, Marvin D, Ponsioen B, Alvarez-Varela A, *et al*. Collagen-rich stroma in aggressive colon tumors induces mesenchymal gene expression and tumor cell invasion. Oncogene 2016;35(40):5263–5271. doi:10.1038/onc.2016.60, PMID:26996663.
[31] Feng H, Zhao JK, Schiergens TS, Wang PX, Ou BC, Al-Sayegh R, *et al*. Bone marrow-derived mesenchymal stromal cells promote colorectal cancer cell death under low-dose irradiation. Br J Cancer 2018;118(3):353–365. doi:10.1038/bjc.2017.415, PMID:29384527.
[32] Dobbin ZC, Landen CN. The importance of the PI3K/AKT/MTOR pathway in the progression of ovarian cancer. Int J Mol Sci 2013;14(4):8213–8227. doi:10.3390/ijms14048213, PMID:23591839.
[33] Jin Q, Liu G, Wang B, Li S, Ni K, Wang C, *et al*. High methionyl-tRNA synthetase expression predicts poor prognosis in patients with breast cancer. J Clin Pathol 2020;73(12):803–812. doi:10.1136/jclinpath-2019-206175, PMID:32404475.
[34] Lv J, Guo L, Wang JH, Yan YZ, Zhang J, Wang YY, *et al*. Biomarker identification and trans-regulatory network analyses in esophageal adenocarcinoma and Barrett's esophagus. World J Gastroenterol 2019;25(2):233–244. doi:10.3748/wjg.v25.i2.233, PMID:30670912.
[35] Zhang Z, Wang Y, Zhang J, Zhong J, Yang R. COL1A1 promotes metastasis in colorectal cancer by regulating the WNT/PCP pathway. Mol Med Rep 2018;17(4):5037–5042. doi:10.3892/mmr.2018.8533, PMID:29393423.
[36] Oleksiewicz U, Liloglou T, Tasopoulou KM, Daskoulidou N, Gosney JR, Field JK, *et al*. COL1A1, PRPF40A, and UCP2 correlate with hypoxia markers in non-small cell lung cancer. J Cancer Res Clin Oncol 2017;143(7):1133–1141. doi:10.1007/s00432-017-2381-y, PMID:28258342.
[37] Zhou ZH, Ji CD, Xiao HL, Zhao HB, Cui YH, Bian XW. Reorganized Collagen in the Tumor Microenvironment of Gastric Cancer and Its Association with Prognosis. J Cancer 2017;8(8):1466–1476. doi:10.7150/jca.18466, PMID:28638462.
[38] Liu J, Shen JX, Wu HT, Li XL, Wen XF, Du CW, *et al*. Collagen 1A1 (COL1A1) promotes metastasis of breast cancer and is a potential therapeutic target. Discov Med 2018;25(139):211–223. PMID:29906404.
[39] Li J, Ding Y, Li A. Identification of COL1A1 and COL1A2 as candidate prognostic factors in gastric cancer. World J Surg Oncol 2016;14(1):297. doi:10.1186/s12957-016-1056-5, PMID:27894325.
[40] Yu PN, Yan MD, Lai HC, Huang RL, Chou YC, Lin WC, *et al*. Downregulation of miR-29 contributes to cisplatin resistance of ovarian cancer cells. Int J Cancer 2014;134(3):542–551. doi:10.1002/ijc.28399, PMID:23904094.
[41] Pires KSN, Gonçalves CM, Botelho RM, Silva ALM, Tenorio LPG, Santos JC, *et al*. Versican is a novel regulator for trophoblast epithelial-mesenchymal transition and invasion. Placenta 2019;83:e27. doi:10.1016/j.placenta.2019.06.090.
[42] Chida S, Okayama H, Noda M, Saito K, Nakajima T, Aoto K, *et al*. Stromal VCAN expression as a potential prognostic biomarker for disease recurrence in stage II-III colon cancer. Carcinogenesis 2016;37(9):878–887. doi:10.1093/carcin/bgw069, PMID:27287872.
[43] Kulbe H, Otto R, Darb-Esfahani S, Lammert H, Abobaker S, Welsch G, *et al*. Discovery and Validation of Novel Biomarkers for Detection of Epithelial Ovarian Cancer. Cells 2019;8(7):E713. doi:10.3390/cells8070713, PMID:31336942.
[44] Ghosh S, Albitar L, LeBaron R, Welch WR, Samimi G, Birrer MJ, *et al*. Up-regulation of stromal versican expression in advanced stage serous ovarian cancer. Gynecol Oncol 2010;119(1):114–120. doi:10.1016/j.ygyno.2010.05.029, PMID:20619446.